

4. Iridium was chemically purified by fusion in Na<sub>2</sub>O<sub>2</sub>, conversion to chlorides, adsorption onto Srafiion NMRR resin [R. A. Nadkarni and G. H. Morrison, *Anal. Chem.* **46**, 232 (1974)], and elution with NH<sub>4</sub>OH. Yields were determined by reactivation.
5. All samples from E13-4 were sieved at 420 μm, and seven samples around the horizon were sieved at 149 μm. Selected samples of the other sections were sieved at 149 μm. Coarse fractions were examined microscopically for the presence of impact melt debris, and its presence was confirmed by electron microprobe analyses.
6. Disconformities are common in sediments at this latitude [M. T. Ledbetter and P. F. Cielski, *Mar. Geol.* **46**, 329 (1982)]. A large disconformity in E13-4 occurs immediately below the impact horizon. Sediments below this disconformity are Eocene zeolitic nannofossil oozes. Our stratigraphic control is insufficient to rule out the possibility that erosion removed the impact horizon from E13-6 and E13-7.
7. The enhanced Ir in E13-1 most likely shares the same impact source as the other cores, but because we did not recover any particles we were unable to confirm that this is the case.
8. J. P. Kennett, *J. Geophys. Res.* **82**, 3843 (1977).
9. C. Junge, *Air Chemistry and Radioactivity* (Academic Press, New York, 1963); S. Glasstone and P. J. Dolan, *The Effects of Nuclear Weapons* (U.S. Department of Defense, Washington, DC, 1977).
10. For vertical incidence and plausible velocities of 15 to 25 km/s, water depths of 10 to 15 times an asteroid diameter are required to bring the projectile to rest [J. D. O'Keefe and T. J. Ahrens, *Lunar Planet. Sci.* **12**, 785 (1981); *Geol. Soc. Am. Spec. Pap.* **190** (1982), p. 103], and the 5-km ocean depth in this region was probably sufficient to prevent the excavation of a crater. The ratio of penetration depth to projectile mass would be lower if the projectile were crushed during atmospheric transit [H. J. Melosh, *Proc. Lunar Planet. Sci. Conf.* **A12**, 29 (1981)]. Another important consideration is the production of shock-vaporized steam [H. J. Melosh, *Geol. Soc. Am. Spec. Pap.* **190** (1982), p. 121], which can shield a projectile from the oceanic lithosphere and can eject water vapor and meteoritic material high into the atmosphere.
11. G. W. Wetherill and E. M. Shoemaker, *Geol. Soc. Am. Spec. Pap.* **190** (1982), p. 1.
12. R. A. F. Grieve, *Annu. Rev. Earth Planet. Sci.* **15**, 245 (1987).
13. B. P. Glass, *Introduction to Planetary Geology* (Cambridge Univ. Press, New York, 1982).
14. G. Kukla, *Quat. Sci. Rev.* **6**, 191 (1987).
15. J. D. Hays and N. D. Opdyke, *Science* **158**, 1001 (1967).
16. T. J. Ahrens and J. D. O'Keefe, *J. Geophys. Res.* **88**, A799 (1983).
17. We are indebted to A. Kaharoodin for the diatom survey. Curation of Eltanin cores is supported by the National Science Foundation. This research was supported by Office of Naval Research grant N00014-87.

16 February 1988; accepted 11 May 1988

## Velocity of Sound and Equations of State for Methanol and Ethanol in a Diamond-Anvil Cell

J. M. BROWN, L. J. SLUTSKY, K. A. NELSON, L.-T. CHENG

The adaptability of laser-induced phonon spectroscopy to the determination of acoustic velocity and the equation of state in the diamond-anvil high-pressure cell is demonstrated. The technique provides a robust method for measurements at high pressure in both solids and liquids so that important problems in high-pressure elasticity and the earth sciences are now tractable. The velocity of sound and the density of methanol at 25°C have been measured up to a pressure of 6.8 gigapascals. These results imply a higher density (by approximately 5 percent) for liquid methanol above 2.5 gigapascals than that given in existing compilations. The adiabatic bulk modulus increases by a factor of 50 at a maximum compression of 1.8. The thermodynamic Grüneisen parameters of methanol and ethanol both increase with increasing pressure, in contrast to the behavior of most solids.

THE COMPRESSION OF MATERIALS AT high pressure allows the study of interatomic interactions in a regime of distances not otherwise easily accessible. Acoustic velocities are directly related to interatomic force constants and these velocities of sound per se are a matter of central importance in the earth sciences. Knowledge of these properties is essential in any chain of reasoning that proceeds from a seismological image of the earth's interior to a geophysical model in terms of density, temperature, and chemical composition. For solids, compression can be determined by x-

ray diffraction although determination of acoustic velocity at very high pressure remains difficult. In the case of liquids and glasses the extended range of pressure and temperature available in the diamond-anvil high-pressure cell has not been extensively exploited for equation of state studies. Laser-induced phonon spectroscopy (1-3) offers an approach to the determination of the dynamical mechanical properties and the equation of state of a crystal or fluid well adapted to the requirements of the diamond-anvil cell. We report a determination of the velocity of sound and the equation of state of liquid methanol from ambient pressure to 6.8 GPa. The pressure dependence of the adiabatic compressibility and the thermodynamic Grüneisen parameter of ethanol have also been determined. We believe that

the method described here will, with some generality, permit investigation of properties of both crystals and fluids, previously accessible with great difficulty, at very high compressions.

The geometry of the experiment is illustrated schematically in Fig. 1. A single 1064-nm pulse, 70 ps in duration, is selected from the output train of a continuously pumped Q-switched and mode-locked Nd-YAG laser and split to create two excitation pulses. These pulses are recombined in the sample. The interference of the intersecting excitation pulses in a nonabsorbing sample results in a spatially periodic stress exerted through electrostriction (impulsive stimulated Brillouin scattering) on the sample. The material response to this spatially periodic, temporally impulsive stress is an acoustic standing wave. If there is an appreciable optical absorption coefficient and rapid radiationless decay of the excited state, sudden spatially periodic heating and thermal expansion (impulsive stimulated thermal scattering) can launch counter-propagating acoustic waves that also contribute to the acoustic amplitude. In methanol and ethanol the thermal pressure generated by the weak absorption associated with the third overtone of the CH stretching mode is the

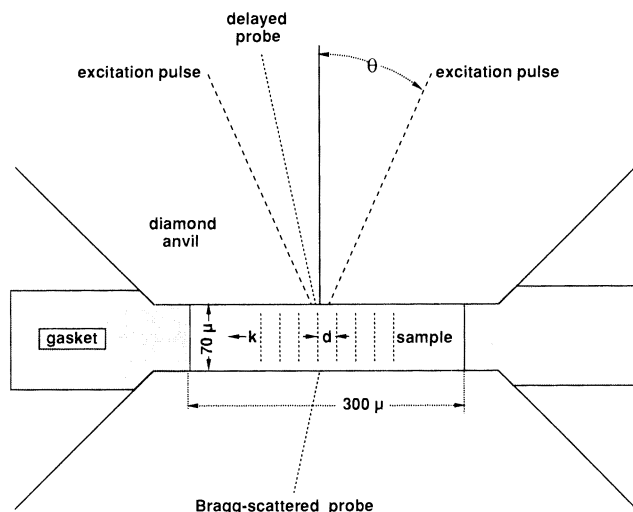
**Table 1.** Velocity of sound, density, adiabatic compressibility, and thermodynamic Grüneisen parameters of methanol and ethanol as a function of pressure at 25°C.

<i>P</i> (GPa)	Veloc- ity (km/s)	$\rho$ (gm/cm <sup>3</sup> )	$K_S$ (GPa)	$\gamma$
<i>Methanol</i>				
0.0001	1.10	0.787	0.96	0.56
0.014	1.18	0.797	1.12	0.60
0.028	1.25	0.808	1.27	0.64
0.041	1.31	0.819	1.41	0.66
0.056	1.37	0.829	1.55	0.68
0.069	1.42	0.836	1.68	0.69
0.083	1.47	0.844	1.82	0.70
0.096	1.51	0.851	1.94	0.71
1.20	2.72	1.074	7.92	0.96
2.07	3.50	1.153	14.20	1.25
2.58	3.76	1.196	16.91	1.35
2.59	3.76	1.196	16.90	1.35
2.92	3.84	1.221	18.03	1.43
4.06	4.53	1.290	26.48	
4.30	4.77	1.303	29.64	
4.89	5.10	1.329	34.69	
6.32	5.53	1.383	42.23	
6.52	5.87	1.390	47.93	
6.82	5.77	1.400	46.57	
<i>Ethanol</i>				
0.0001	1.15	0.785	1.03	0.59
0.58	2.09	0.983	4.29	0.75
1.32	2.86	1.085	8.88	0.99
1.35	3.08	1.087	10.3	1.14
1.90	3.39	1.138	13.0	1.16
2.12	3.40	1.158	13.7	1.12
2.20	3.57	1.165	14.8	1.17
3.19	3.97	1.241	19.6	1.17

J. M. Brown, Geophysics Program, and L. J. Slutsky, Department of Chemistry, University of Washington, Seattle, WA 98195.

K. A. Nelson and L.-T. Cheng, Department of Chemistry, Massachusetts Institute of Technology, Cambridge, MA 02139.

**Fig. 1.** The geometry of laser-induced phonon spectroscopy in a diamond-anvil cell. The angle between excitation pulses is  $2\theta$ . The variably delayed probe pulse is Bragg-diffracted by the ultrasonic standing wave to generate the signal.



principal contributor to the excitation of ultrasonic waves.

The ultrasonic wavelength,  $d$ , and wave vector,  $\mathbf{k}$ , in terms of  $\lambda$  (the wavelength of the laser light) and  $\theta$  (defined in Fig. 1) are given by

$$d = |\mathbf{k}|^{-1} = \frac{\lambda}{2\sin\theta} \quad (1)$$

Since  $\lambda$  and  $\sin\theta$  are both inversely proportional to the index of refraction of the sample, their values in air can be used in Eq. 1 to calculate the acoustic wavelength. That the determination of the velocity is independent of the index of refraction of the medium is a significant amenity of this technique.

A subsequent pulse in the output train is frequency-doubled and delayed by variation of the optical path to serve as a probe. Observation of the intensity of the Bragg scattering of the delayed probe from the acoustic grating as a function of the delay permits the determination of the frequency (or frequencies),  $\nu$ , and hence the velocity,  $u$ , of the acoustic wave, since  $u = d\nu$ . In these experiments a beam diameter of  $\approx 200 \mu\text{m}$  in the scattering plane and scattering angles of about  $10^\circ$  are employed. Pressure is measured by ruby fluorescence excited by a continuous-wave HeCd laser (4).

Time-domain data for the intensity of the Bragg-scattered probe pulse are shown in Fig. 2. The increase in sound velocity associated with the increase in pressure is apparent in the decreasing period of the acoustic standing wave. The signal envelope is primarily caused by acoustic wave propagation beyond the probed area. Sound velocities for methanol and ethanol, determined from the frequencies and wavelengths of the acoustic standing waves, are listed in Table 1. Under ideal conditions, uncertainties in velocities are typically of order 0.3% (5). In the present work the limited number of observed wave cycles and room temperature

fluctuations generate uncertainties in acoustic frequencies of order 1%.

The equation of state can be deduced from the experimentally determined velocity of sound,  $u$ , and the known density,  $\rho$ , at ambient pressure by integration of

$$\begin{aligned} \left(\frac{\partial \rho}{\partial P}\right)_T &= \left(\frac{\partial \rho}{\partial P}\right)_S + \alpha\rho\left(\frac{\partial T}{\partial P}\right)_S \\ &= u^{-2} + \alpha\rho\left(\frac{\partial T}{\partial P}\right)_S \end{aligned} \quad (2)$$

where  $\rho$  is the density,  $\alpha$  is the coefficient of thermal expansion,  $P$  is pressure,  $T$  is temperature, and  $S$  is entropy. The adiabatic bulk modulus is calculated from the density and velocity of sound

$$K_S = \rho u^2 = \left(\frac{\partial P}{\partial \ln \rho}\right)_S \quad (3)$$

The room temperature isotherm for methanol up to 6.82 GPa, which is based on integration of the diamond-anvil acoustic velocity measurements starting from the density measured by Bridgman (6) at 1.96 GPa, is given in Fig. 3 (7). This isotherm is compared with Bridgman's results between 1.96 and 4.9 GPa. Bridgman construed the lack of agreement between two sets of measurements above 2.45 GPa as evidence for supercooling and plausibly selected the lower density series of observations as representative of the properties of the metastable liquid. It is now established that, although methanol metastably compresses to a glass transition at 8.6 GPa, the equilibrium freezing point at  $25^\circ\text{C}$  is approximately 3.58 GPa (8). An alternative explanation for Bridgman's results (6) must then be sought.

The diamond-anvil isotherm is, by direct observation, that of the metastable liquid. This isotherm is in good agreement with Bridgman's results (6) at the pressures at which the piston-cylinder experiments have

proven reproducible. The present liquid isotherm agrees well with the higher density series of measurements (construed by Bridgman as representing the solid phase of methanol) in the range of pressure accessible to both techniques, and extends isothermal compression data to significantly higher pressures.

The densities given in Fig. 3, together with the velocities measured here and those determined by Wilson and Bradley (9) below 0.1 GPa permit the calculation of the adiabatic bulk modulus (Table 1). The variation in  $K_S$  is considerable, the value at 6.82 GPa being almost 50 times that at 1 atm. The compressions and moduli of ethanol and methanol are almost identical. Boehler and Kennedy (10) have measured  $(\Delta T/\Delta P)_S$  for both methanol and ethanol from 1 atm to 2.4 GPa. The thermodynamic Grüneisen parameter, defined by  $\gamma = \alpha K_S/C_p\rho$ , is calculated from  $\gamma = K_S T^{-1}(\Delta T/\Delta P)_S$ . Thermodynamically,  $\gamma$  is the inverse of the derivative of the energy density with respect to pressure at constant volume. In the case of solids  $\gamma$  may be interpreted as the mean

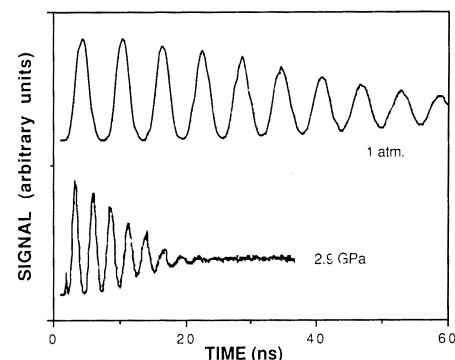


**Fig. 2.** Time-domain diffraction data for methanol in a diamond-anvil high-pressure cell. At room pressure data were obtained with  $\theta$  equal to  $4.5^\circ$ ; at 2.9 GPa,  $\theta$  was  $3^\circ$ .

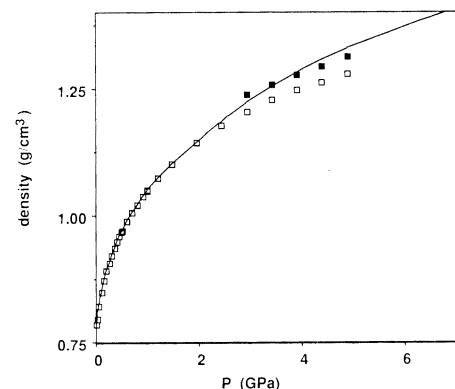


**Fig. 3.** Density of liquid methanol at 298 K as a function of the pressure. The solid curve is the result of the integration of Eq. 2, presuming Bridgman's value at 1.96 GPa. The open and filled squares represent Bridgman's results.

logarithmic derivative of phonon frequency with respect to uniform strain, that is,  $\gamma = (\partial \ln \nu / \partial \ln V)_k$ .

For a variety of liquids, the pressure-dependence of  $(\Delta T / \Delta P)_S$  at high pressure is small. The calculation of  $\gamma$  in Table 1 is therefore extended by extrapolation to 2.9 GPa of results up to 2.4 GPa. As for the other liquids where the isothermal pressure-dependence of  $\gamma$  is known [Hg, water, pentane, and isopentane (10)], in contrast to solids (11) and Earth's mantle and core (12), the Grüneisen parameters of ethanol and methanol increase with decreasing volume.

It is the evaluation of the second term on the right side of Eq. 2, the "correction" of the experimentally determined adiabatic compressibility to the isothermal compliance  $[K_S^{-1} = K_T^{-1} - \alpha(\partial T / \partial P)_S]$ , that constitutes the principal source of uncertainty in this preliminary study. The direct measurement of  $(\Delta T / \Delta P)_S$  by Boehler and Kennedy (10) and the classical study of the  $P$ - $V$ - $T$  relations of methanol by Bridgman (6) do, however, serve to determine this correction over the range of pressure wherein it is large (Fig. 4) and provide a basis for the deduction of the pressure-volume relations at higher pressures. The experimental pressure-dependence of the correction and the smooth curve used in the integration of Eq. 2 are given in Fig. 4.

The correction term in Eq. 2 can also be expressed as  $\alpha^2 T / C_p$ . The pressure dependence of this quantity is implicit in the  $P$ - $V$ - $T$  relations and so may be approximated recursively from sound velocity data at a series of temperatures (13). Thus, laser-induced phonon spectroscopy in the diamond-anvil cell offers an approach to the determination of acoustic velocities and the

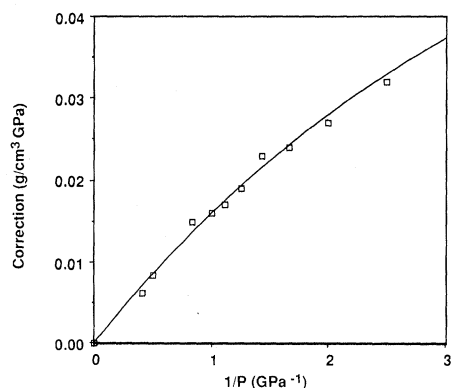


**Fig. 4.** The second term in Eq. 2 (that is, the density times the difference between the isothermal and adiabatic compressibilities) calculated from  $(\Delta T / \Delta P)_S$  (10) and the coefficient of thermal expansion (6), plotted with open squares, and extrapolated (solid curve) to higher pressures. The estimated uncertainty in the correction is comparable with the scatter of the experimental points.

equation of state at high compression. In these preliminary studies we have sought to compare the results obtained at the lower end of the range conveniently investigated in the diamond-anvil cell with those obtained by other techniques and to extend the equation of state of methanol to higher compressions than have been investigated by the conventional piston-cylinder techniques. The technique reported here should be quite generally applicable. We have, for example, observed strong scattering from thermally excited quasilongitudinal and quasitransverse waves in olivine at high pressure (5). As another example, less than 0.5% water produces a useful signal from  $N_2$  in the diamond-anvil cell.

#### REFERENCES AND NOTES

1. Y. X. Yan, L. T. Cheng, K. A. Nelson, in *Advances in Non-linear Spectroscopy*, J. H. Clark and R. E. Hester, Eds. (Wiley, London, 1987), pp. 299-354.
2. M. D. Fayer, *Annu. Rev. Phys. Chem.* **33**, 63 (1982).
3. K. A. Nelson, R. J. D. Miller, D. R. Lutz, M. D. Fayer, *J. Appl. Phys.* **53**, 1144 (1982).
4. H. K. Mao and P. M. Bell, *ibid.* **49**, 3276 (1978).
5. J. M. Brown, L. J. Slutsky, K. A. Nelson, L.-T. Cheng, in preparation.
6. P. W. Bridgman, *Proc. Am. Acad. Arts Sci.* **74**, 403 (1942); *International Critical Tables* (McGraw-Hill, New York, 1928), vol. 3, p. 41.
7. We initiate the integration at 1.96 GPa because (i) Bridgman's data are quite accurate at and below this pressure range and (ii) integration with sparse data at the lowest pressures (where velocities increase rapidly with pressure) tended to be unstable.
8. G. J. Piermarini, S. Block, J. D. Barnett, *J. Appl. Phys.* **44**, 5377 (1973).
9. W. Wilson and D. Bradley, *J. Acoust. Soc. Am.* **36**, 333 (1964).
10. R. Boehler and G. C. Kennedy, *J. Appl. Phys.* **48**, 4183 (1977).
11. R. Boehler and J. Ramakrishnan, *J. Geophys. Res.* **85**, 6696 (1980).
12. J. M. Brown and T. J. Shankland, *Geophys. J. R. Astron. Soc.* **66**, 579 (1981).
13. R. L. Mills, D. H. Liebenberg, J. C. Bronson, *J. Chem. Phys.* **63**, 1198 (1975).
14. This work was supported by NSF grants DMR-8704352 (K.A.N. and L.-T.C.) and EAR-8618573 (J.M.B. and L.J.S.).

22 March 1988; accepted 24 May 1988

## Brownian Dynamics of Cytochrome c and Cytochrome c Peroxidase Association

SCOTT H. NORTHRUP,\* JEFFREY O. BOLES, JOHN C. L. REYNOLDS

Brownian dynamics computer simulations of the diffusional association of electron transport proteins cytochrome c (cyt c) and cytochrome c peroxidase (cyt c per) were performed. A highly detailed and realistic model of the protein structures and their electrostatic interactions was used that was based on an atomic-level spatial description. Several structural features played a role in enhancing and optimizing the electron transfer efficiency of this reaction. Favorable electrostatic interactions facilitated long-lived nonspecific encounters between the proteins that allowed the severe orientational criteria for reaction to be overcome by rotational diffusion during encounters. Thus a "reduction-in-dimensionality" effect operated. The proteins achieved plausible electron transfer orientations in a multitude of electrostatically stable encounter complexes, rather than in a single dominant complex.

**B**IOLICAL PROCESSES ON A MOLECULAR level require the transport of reactants through space by a diffusional mechanism leading to a reactive event (1). In many cases the diffusional encounter of species limits the overall rate, and thus a knowledge of the dynamics of such encounters is of fundamental importance in the understanding of the biological event. Usually, one or more of the species is a macromolecule having a small reactive region relative to its overall size, which can lead to very severe orientational criteria for reaction. Adam and Delbruck (2) proposed that in order to overcome the formidable obstacle posed by the required translational and rotational search process, the efficiency of biochemical systems may be optimized by exploiting the so-called reduction-in-dimensionality principle, in which the molecular

species diffuse in a three-dimensional space and initially associate in unreactive configurations by ubiquitous nonspecific forces of attraction, either of a Coulombic or van der Waals type. This association is followed by a diffusional search on a lower dimensional configurational surface of associated particles that increases the probability of ultimate production of a properly oriented pair. The magnitude of forces promoting the initial nonspecific association must be finely tuned to a range allowing particles to remain in juxtaposition for time scales required for the lower dimensional diffusive search, but not so strong that encountered particles are locked into unproductive orientations. This

Department of Chemistry, Tennessee Technological University, Cookeville, TN 38505.

\*To whom correspondence should be addressed.